TABLE III. Percent conversion to Fe(II). Pressure (kbar).

Derivative	40	60	80	100	120	140	160	180[a]
				Class A				
ACA(1)	16.4	29.7	44.3	57.9	67.7	73.3	75.7	76.4
BA(4)	18.3	30.1	42.2	54.0	65.3	73.5	77.1	77.5
TFACA(5)	13.8	20.8	29.6	45.5	60.4	67.6	70.0	70.5
MACA(9)	20.3	35.6	51.1	62.2	67.9	71.1	73.1	74.5
NACA(11)	7.1	21.7	38.2	52.0	59.2	61.8	62.4	62.4
EACA(12)	34.0	48.9	59.3	67.0	72.8	76.6	78.5	78.8
				Class B				
FTFA(6)	17.0	35.0	50.4	58.3	61.4	62.0	62.0	62.0
TTFA(7)	5.3	23.6	41.4	55.3	63.8	66.5	67.0	67.0
BTFA(8)	7.0	25.2	41.6	54.4	62.5	66.2	67.0	67.0
PACA(10)	9.4	21.1	37.4	53.2	60.5	64.2	65.0	65.0
				Class C				
DBM(2)	25.2	42.5	52.0	55.6	56.7	57.0	57.0	57.0
DPM(3)	39.0	48.6	55.8	60.5	63.8	66.0	67.2	67.5

[a] Extrapolated values.

of Class A at higher pressures. This is analogous to the behavior of its Fe(II) isomer shift.

The smoothed curves for Class B are shown in Fig. 9. The atmospheric and low pressure behavior of the three fluorinated derivatives FTFA(6), TTFA(7), and BTFA(8) are very similar, with the fairly high values (0.45–0.46 mm/sec) predominantly due to the presence of the electronegative trifluoromethyl group. There is no tendency toward maxima in the low pressure region for these three derivatives. This is consistent with the assumption that the trifluoromethyl group reduces the initial 4*s* augmentation to very small values. However, in contrast to the large TFACA(5) isomer shift decrease of 0.16 mm/sec over the whole pressure range, TTFA(7) and BTFA(8) show much smaller decreases of 0.07 and 0.08 mm/sec, respectively. FTFA(6) shows an increase at higher pressures. The similar behavior of TTFA(7) and BTFA(8) is reasonable on the basis of the structure of the second terminal substituent, where the sulfur in the heterocyclic thiophene ring of TTFA(7) has the same Pauling electronegativity as carbon in the phenyl ring of BTFA(8). The fourth member of the class, PACA(10), also exhibits only a rather small decrease in isomer shift above 50 kbars.

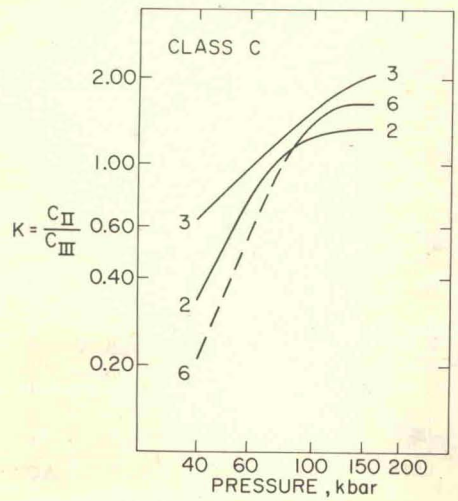

FIG. 14. Log K vs log P—Class C.

It has been already noted that, on the basis of Fe(II) isomer shifts, these derivatives show extensive backbonding in the ferrous state. Backbonding would be expected for the ferric state also but in general this state has less than the ferrous state. The relatively small decreases in isomer shift may then be associated with a decrease in backbonding with pressure such as that observed in phenanthroline complexes and some ferrocyanides.[5,9,33]

PACA(10) shows typical Class B behavior above 50 kbars with a rather slight decrease in Fe(III) isomer shift. However, it is distinguished by the very large increase in isomer shift in the low pressure region. Such an increase is similar in form, if not in degree, to those observed in several Class A derivatives. The 4*s* augmentation argument should apply but it seems unlikely to be the only effect as the increase is so large. The answer may lie in one of the contributions of symmetry restricted covalency to the isomer shift, e.g., involving overlap of ligand electron density in the metal bond region. If the ligand overlap should extend inside the 3*s* orbital, the isomer shift will increase due

TABLE IV. Equilibrium constant parameters.

Derivative	A	M	Pressure range
	Class A		
ACA(1)	5.82×10^{-5}	2.18	40–150
BA(4)	5.30×10^{-5}	2.19	55–165
TFACA(5)	2.18×10^{-6}	2.80	65–140
MACA(9)	2.06×10^{-4}	1.94	40–120
NACA(11)	2.46×10^{-6}	2.83	40–110
EACA(12)	1.88×10^{-3}	1.52	40–150
	Class B		
FTFA(6)	2.69×10^{-5}	2.42	40–85
TTFA(7)	3.61×10^{-6}	2.76	50–120
BTFA(8)	5.91×10^{-6}	2.65	50–115
PACA(10)	3.09×10^{-6}	2.78	45–115
	Class C		
DBM(2)	2.64×10^{-4}	1.94	40–75
DPM(3)	1.70×10^{-2}	0.98	40–120

to the resulting shielding of the 3s. Of course one would expect pressure to increase such overlap generally for all the derivatives but the effect may not be important unless there is appreciable initial steric hindrance. There is ample evidence that the phenyl ring in PACA(10) is not coplanar with the chelate ring as a result of steric inhibition. Thus it seems possible that the additional crowding would lead to greater ligand overlap and hence an increase in isomer shift.

The Fe(III) isomer shifts for Class C, consisting of DBM(2) and DPM(3), are shown in Fig. 10. Low pressure data are difficult to obtain because of the very low percent effect and the non-Lorentzian broadening referred to earlier. (This broadening diminishes with increasing pressure and becomes insignificant above 70 kbars.) However, it appears that both isomer shifts are rather low, in the region of 0.25 mm/sec. The low values probably arise from different effects with extensive d_π delocalization to the two aromatic rings predominating in DBM(2) and appreciable σ donation from the tertiary butyl groups in DPM(3). The important feature is that both derivatives show quite large increases in Fe(III) isomer shift so that at the highest pressure the values range between 0.52–0.55 mm/sec. As already mentioned, FTFA(6) also shows an increase in isomer shift in the high pressure region qualitatively similar to DBM(2) and DPM(3). The increase in isomer shift may be explained in part by the reduction of backbonding and 4s occupation with pressure for DBM(2) and DPM(3), respectively. In addition, there are probably contributions due to 3s shielding arising from overlap with occupied ligand orbitals.

Reduction of Fe(III) *to* Fe(II)

We turn now to a discussion of the reduction of Fe(III) to Fe(II). The general characteristics of this process have been presented earlier. We emphasize here the correlation with electronic properties. Typical conversion data in the form of log$K$ are plotted as a function of log$P$ for ACA(1) in Fig. 11. The linear plot holds over a considerable pressure range. The deviations at low pressure may be associated with difficulties in measuring conversions below 10%. High pressure deviations are discussed below.

Smoothed conversion data for Classes A, B, and C are shown in terms of equilibrium constant plots in Figs. 12, 13, and 14 with the tabulated conversions given in Table III. The constants A and M in the empirical relation for the equilibrium constant $K=AP^M$ are given in Table IV. The conversion behavior of the three classes provides further justification for the classification scheme. For example, Class A derivatives show continuously increasing conversion over the whole pressure range. Furthermore, the linear behavior is obtained over a substantial portion of the range, with an upper limit between 140–165 kbars for ACA(1), BA(4), TFACA(5), and EACA(12). MACA(9) appears to show a change of slope at about 110 kbars but increases steadily thereafter. On the other hand, NACA(11) tends to level off at high pressures.

Class B derivatives show linear behavior between roughly 45–115 kbars and show distinct tendencies to level off and become independent of pressure above 150 kbars. The only exception to this behavior is shown by FTFA(6) which appears to exhibit Class B properties in the low pressure region but Class C behavior at high pressure. The slopes of the conversion curves in the linear region are very similar with TTFA(7),

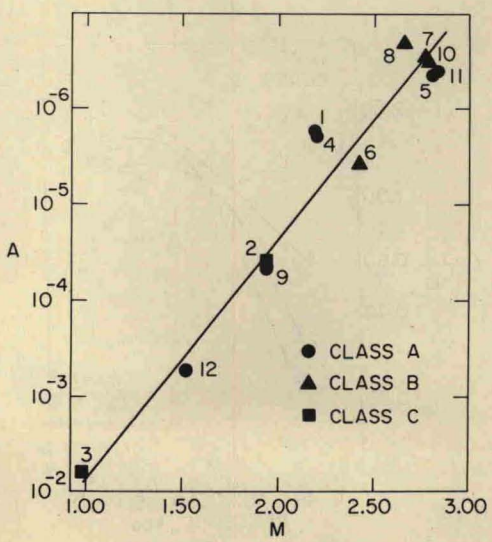

FIG. 15. Log A vs M—all compounds.